

# Journal Pre-proof

Hierarchical Beta zeolites obtained in concentrated reaction mixtures as catalysts in tetrahydropyranlation of alcohols

Roman Barakov, Nataliya Shcherban, Pavel Yaremov, Igor Bezverkhy, Valentina Tsyryna, Maksym Opanasenko



PII: S0926-860X(19)30535-6  
DOI: <https://doi.org/10.1016/j.apcata.2019.117380>  
Reference: APCATA 117380

To appear in: *Applied Catalysis A, General*

Received Date: 21 October 2019  
Revised Date: 7 December 2019  
Accepted Date: 17 December 2019

Please cite this article as: Barakov R, Shcherban N, Yaremov P, Bezverkhy I, Tsyryna V, Opanasenko M, Hierarchical Beta zeolites obtained in concentrated reaction mixtures as catalysts in tetrahydropyranlation of alcohols, *Applied Catalysis A, General* (2019), doi: <https://doi.org/10.1016/j.apcata.2019.117380>

This is a PDF file of an article that has undergone enhancements after acceptance, such as the addition of a cover page and metadata, and formatting for readability, but it is not yet the definitive version of record. This version will undergo additional copyediting, typesetting and review before it is published in its final form, but we are providing this version to give early visibility of the article. Please note that, during the production process, errors may be discovered which could affect the content, and all legal disclaimers that apply to the journal pertain.

© 2019 Published by Elsevier.

## Hierarchical Beta zeolites obtained in concentrated reaction mixtures as catalysts in tetrahydropyranylation of alcohols

Roman Barakov<sup>a,b</sup>, Nataliya Shcherban<sup>b</sup>, Pavel Yaremov<sup>b</sup>, Igor Bezverkhyy<sup>c</sup>, Valentina Tsyryna<sup>b</sup>, Maksym Opanasenko<sup>a\*</sup>

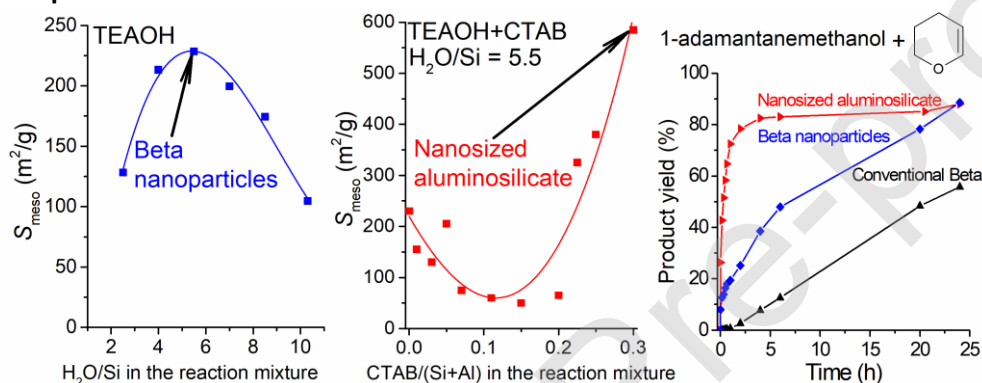
<sup>a</sup>Department of Physical and Macromolecular Chemistry, Faculty of Science, Charles University in Prague, Hlavova 2030, 12840 Prague 2, Czech Republic

<sup>b</sup>L.V. Pisarzhevsky Institute of Physical Chemistry, National Academy of Sciences of Ukraine, 31 pr. Nauky, Kiev, 03028, Ukraine

<sup>c</sup>Laboratoire Interdisciplinaire Carnot de Bourgogne, UMR 6303 CNRS-Université de Bourgogne-Franche Comté, 9 Av. A. Savary, BP 47870, 21078, Dijon Cedex, France

\*Corresponding author: maksym.opanasenko@natur.cuni.cz

### Graphical abstract



### Highlights

- Hierarchical zeolites consisting of Beta nanoparticles were obtained via hydrothermal treatment of the concentrated mixtures ( $\text{H}_2\text{O}/\text{Si} = 2.5 - 14$ ).
- An optimal  $\text{H}_2\text{O}/\text{Si}$  ratio in the mixture for obtaining of hierarchical Beta zeolites with the high accessibility of the acid sites for bulky molecules is 5.5.
- The use of CTAB additionally limits the crystallite growth and promotes the formation of highly porous nanosized aluminosilicate.
- Hierarchical Beta zeolites obtained in the concentrated mixtures demonstrate high catalytic activity in the reaction of bulky alcohols with 3,4-dihydro-2H-pyran.

### Abstract.

Hierarchical zeolites consisting of Beta nanoparticles (15 – 40 nm) were obtained via hydrothermal treatment of a concentrated zeolite gel-precursor ( $\text{H}_2\text{O}/\text{Si} = 2.5 - 14$ ) without utilization of complex SDAs. The proposed approach is based on the formation of a large number of zeolite nuclei under particular crystallization conditions, followed by their agglomeration resulting in the dense packing of the particles preventing their further growth. The micelles of cetyltrimethylammonium bromide (CTAB) can be used to additionally limit the growth of zeolite nanoparticles during hydrothermal

treatment of concentrated reaction mixtures. Such deceleration of crystallization promotes the formation of highly porous X-ray amorphous nanosized aluminosilicate. Due to the developed mesoporosity and increased accessibility to the acid sites for the molecules of a large size, hierarchical Beta zeolites obtained in the presence of CTAB demonstrate high catalytic activity in the reaction of bulky alcohols (1-octadecanol and 1-adamantanemethanol) with 3,4-dihydro-2H-pyran.

**Keywords:** Hierarchical Beta zeolite; Concentrated reaction mixture; Cetyltrimethylammonium bromide; Accessible acid sites; Tetrahydropyranlation of alcohols.

## 1. Introduction

Search and development of the methods for the synthesis of hierarchical zeolites is one of the most actual problem in the field of zeolite-like materials [1–6]. These materials to a certain extent combine the properties of zeolites and mesoporous molecular sieves, in particular, contain strong acid sites and mesopores, which improve diffusion and promote accessibility of catalytic sites [7,8]. As a result, hierarchical zeolites are promising catalysts for reactions involving bulky organic molecules, especially in the production of fine chemicals and biomass transformation [9,10].

One of the possible pathways to obtain hierarchical zeolites is the assembly of zeolite nanoparticles to the material possessing interparticle mesopores [11]. Such materials can be prepared in the presence of hard templates (for example, carbon nanoparticles, polystyrene spheres) [12], non-ionic (polyvinyl alcohol [13]) and cationic polymers (dimethyldiallyl ammonium chloride acrylamide copolymer [14]), as well as multi-quaternary ammonium surfactants, which are able to direct the formation of both zeolite and mesoporous structures [15,16]. The surfactant (e.g. cetyltrimethylammonium bromide, CTAB) micelles can also limit the growth of zeolite nanoparticles during gel crystallization that allows to obtain hierarchical Beta zeolite with well-developed mesoporosity. In the dual template method, reaction mixture (RM) containing both zeolite structure-directing agent (e.g. tetraethylammonium hydroxide, TEOH) and surfactant (CTAB) can be used to prepare either Beta/MCM-41 composites or agglomerates of Beta zeolite nanoparticles depending on the aging time [17].

Assemblies of zeolite nanoparticles can also be obtained without additional mesoporegens by the careful choice of the synthesis conditions (composition and pH of the RM, temperature and duration of hydrothermal treatment (HTT)) [18,19] or using the “dry gel” conversion techniques [20–23]. During HTT or steam assisted conversion of highly concentrated zeolite gel-precursor, a large amount of zeolite nuclei is rapidly formed with a subsequent crystallization and assembly in zeolite nanoparticles agglomerates [21,24,25]. However, mentioned methods for obtaining of hierarchical nanoparticles assemblies with the use of highly concentrated RM have several drawbacks such as relatively broad mesopore size distribution, low crystallinity, and limited concentration of strong Brønsted acid sites in the obtained aluminosilicates. It can be assumed, that the further optimization of the concentrated mixture composition and the synthesis conditions, as well as the use of surfactant additives will allow to improve the corresponding characteristics of the materials. The understanding of the influence of the RM composition (in particular H<sub>2</sub>O/Si ratio), duration and temperature of HTT on the textural, acid and catalytic properties of aluminosilicates consisting of zeolite nanoparticles agglomerates, as well as the role of surfactant additives (CTAB) in hierarchical zeolites formation process is crucial for the development of the synthesis methods

based on the use of concentrated RM, which allow to adjust the textural and acid properties of the mentioned aluminosilicates.

The aim of this study was to determine the features of hierarchical Beta zeolites formation in concentrated RMs, as well as to investigate the influence of the RM composition ( $H_2O/Si$  and  $CTAB/(Si+Al)$  ratios) and the synthesis conditions (duration of HTT) on the structure, acid properties and catalytic activity of the obtained hierarchical zeolites. The catalytic behavior of the designed materials was also compared with that of conventional microporous and nanosponge Beta zeolites. The latter hierarchical zeolite synthesized in the presence of multi-quaternary ammonium surfactant  $[C_{22}-6Npipe-C_{22}](OH)_6$  [26] is especially important reference material because it is composed of nanoparticles assemblies similarly to the materials investigated in this work, but its preparation is significantly more costly.

## 2. Experimental part

### 2.1 Synthesis of the samples

Hierarchical Beta zeolites (MB – mesoporous Beta) were obtained via hydrothermal treatment of a concentrated Beta zeolite gel-precursor ( $H_2O/Si = 2.5 - 14$ ). Zeolite Beta gel-precursor ( $Si/Al = 25$ ) was synthesized according to the technique similar to that given in Ref. [27]. Tetraethylammonium hydroxide solution (40 %, SACHEM, Inc., 5.3 ml) and 0.4 ml of HCl (35 wt%) were added to 4.8 ml of  $H_2O$ . Then 1.479 g of  $SiO_2$  (Aerosil A-175) was added under vigorous stirring. After stirring for 30 min, 0.515 g of as-synthesized aluminum hydroxide (9.8 wt%  $Al_2O_3$ ) and 0.057 g of NaOH (Lach-Ner, 99 %) were added and the reaction mixture was stirred for 1 h. Then obtained RM (composition:  $1SiO_2:0.02Al_2O_3:0.028Na_2O:0.6TEAOH:0.2HCl:20H_2O$ ) was dried at 75 °C to  $H_2O/Si$  molar ratio in the gel 1 – 14 (Table 1, see Table S1 for full details). For obtaining of hierarchical zeolites, the samples in a teflon liners were placed in an autoclave and subjected to HTT at 140 °C for 1 – 9 days (samples MB-1 – 12). The reference sample of Beta zeolite (CB-1 – conventional Beta) was obtained by HTT of zeolite-forming RM ( $Si/Al = 35$ ) at 140 °C for 7 days without preliminary drying.

**Table 1**

Synthesis conditions and degree of crystallinity of the samples.

Sample	$H_2O/Si$ molar ratio	$\tau^a$ (days)	$CTAB/(Si+Al)$ molar ratio	The degree of crystallinity
MB-1 – 5	2.5	1 – 9	–	0.15 – 1.0
MB-6 – 12	1 – 14	7	–	0.6 – 1.0 <sup>b</sup>
MB-13 – 22	5.5	7	0.01 – 0.30	0.55 – 0.90 <sup>b</sup>
CB-1	20	7	–	0.60

<sup>a</sup>  $\tau$  is the duration of hydrothermal treatment.

<sup>b</sup> Samples MB-6 and MB-21, 22 are amorphous.

Hierarchical zeolites were also prepared in the presence of CTAB. For this, surfactant solution was preliminary prepared. In a typical synthesis by the general technique, 0.097 g of CTAB, Sigma,  $\geq 98$  % (at  $CTAB/(Si+Al)$  ratio of 0.01) was added to an aqueous solution of sodium

hydroxide (0.051 g of NaOH was dissolved in 4.4 ml of H<sub>2</sub>O) and stirred at 30 °C for 30 min. Then an alkaline surfactant solution was added to the Beta zeolite gel-precursor and the mixture was stirred for 1 h at the room temperature. The obtained reaction mixture (composition 1SiO<sub>2</sub>:0.02Al<sub>2</sub>O<sub>3</sub>:0.053Na<sub>2</sub>O:0.6TEAOH:0.01CTAB:0.2HCl:30H<sub>2</sub>O) was dried at 75 °C to H<sub>2</sub>O/Si molar ratio in the gel 5.5 (Table 1). The concentration of CTAB in the reaction mixture was varied according to the CTAB/(Si+Al) ratio of 0.03 (H<sub>2</sub>O/Si = 30 – in the initial RM), 0.05 (30), 0.07 (30), 0.11 (40), 0.15 (40), 0.20 (40), 0.225 (40), 0.25 (40), 0.30 (60). The samples in a teflon liner were placed in an autoclave and subjected to HTT at 140 °C for 7 days (samples MB-13 – 22).

Hierarchical Beta zeolite (NS-1 – nanosponge Beta) was also synthesized in the presence of the multi-quaternary ammonium surfactant [C<sub>22</sub>-6Npipe-C<sub>22</sub>](OH<sup>-</sup>)<sub>6</sub> according to the technique given in Ref. [26]. Tetraethylortosilicate (TEOS, Aldrich, 98 %) and aluminum isopropoxide (Aldrich, ≥ 98 %) were used as silicon and aluminum sources respectively (Si/Al = 15 in the RM). For obtaining the hierarchical zeolite, the RM (1SiO<sub>2</sub>:0.033Al<sub>2</sub>O<sub>3</sub>:0.06[C<sub>22</sub>-6Npipe-C<sub>22</sub>](OH<sup>-</sup>)<sub>6</sub>:167H<sub>2</sub>O) was subjected to HTT at 140 °C for 12 days.

Commercial Beta zeolite with the Si/Al ratio (in the sample) of 19 (CB-2, NH<sub>4</sub><sup>+</sup>-form) was also used as the reference sample. This zeolite was supplied by Zeolyst International Company.

All obtained samples of MB and sample CB-1 (in Na-form) were washed with distilled water, dried at 100 °C and calcined in air at 550 °C for 5 h (heating rate was 2 °C/min). After calcination the samples were subjected two times to ion-exchange in 1 M NH<sub>4</sub>Cl solution at 40 °C for 24 h to obtain NH<sub>4</sub><sup>+</sup>-form, which then was converted to H-form by a standard procedure (heating to 550 °C with the rate 2 °C/min, holding time was 5 h). The samples CB-2 and NS-1 (after washing and drying) directly calcined in air at 550 °C for 5 h to obtain H-form of the samples.

## 2.2 Characterisation of samples

Phase composition of the obtained samples was analyzed using X-ray diffractometer D8 ADVANCE (Bruker AXS) with CuK<sub>α</sub>-radiation. An average Beta crystallite size (average size of coherent scattering regions) was calculated by the Scherrer's equation. This equation is used to estimate crystallite size from 1.5 – 2 nm to 0.2 μm (error ~20 %) [28]. According to the technique given in Ref. [18], the degree of crystallinity ( $\alpha_{\text{cryst}}$ ) was evaluated by change in the ratio of the area under the peaks in the  $2\theta = 20 - 24^\circ$  range in the XRD pattern of the investigated samples and the sample MB-9 with the largest area in this range, for which the degree of crystallinity was accepted as one. The calculations of crystallite size and  $\alpha_{\text{cryst}}$  were given for the calcined samples.

FTIR spectra of the as-synthesized samples (pellet with KBr, 1: 100) were measured on the Fourier spectrometer Spectrum One (Perkin Elmer).

The content of Si and Al in the obtained samples was determined by energy dispersive X-ray spectroscopy (the MIRA-3 instrument).

SEM images of the samples were obtained using field emission SEM MIRA-3 (Tescan). Images were recorded using the accelerating voltage of 1 – 30 kV and a secondary electron detector. The sample was loaded on the conductive graphitized support and recording carried out without preliminary deposition of conductive materials on the sample surface. TEM images were obtained using field emission TEM JEM-2100F (JEOL) with an accelerating voltage of 200 kV. The samples were dispersed in ethanol in an ultrasonic bath for 5 min, and then the suspension was deposited onto a copper grid coated with an amorphous carbon film.

Nitrogen adsorption was measured by volumetric method (77 K, up to 1 atm) on the analyzer of porous materials Sorptomatic 1990 (Thermo Electron Corp.). Prior to measurements samples were evacuated ( $P \leq 0.7$  Pa) at 350 °C for 5 h. Specific surface area  $S_{\text{BET}}$  was evaluated by BET equation; the micropore size was calculated by the method of Saito-Foley; the mesopore size was determined from the desorption branch of the isotherm, using the method of Barret-Joyner-Hallenda (BJH). The micropore and mesopore volumes as well as mesopore surface area (including also the external surface area) were determined by the comparative *t-plot* method.

Solid-state  $^{27}\text{Al}$  MAS NMR spectra were obtained using an Avance III HD (Bruker) spectrometer working with a 9.4 T standard-bore superconducting magnet ( $^{27}\text{Al}$  Larmor frequency of 104.26 MHz). The samples were packed into a thin-wall 3.2 mm zirconia rotor, and rotated at a MAS rate of 15 kHz using a Bruker 3.2 mm HX CP-MAS probe. A pulse of 1.0  $\mu\text{s}$  (B1 field approx. 95 kHz) with a relaxation delay of 1 s was applied and 2048 transients were averaged. The spectra were referenced to saturated solution of  $\text{Al}(\text{NO}_3)_3$  in  $\text{D}_2\text{O}$ . In all cases, no proton decoupling was applied.

The method of pyridine ad(de)sorption with IR-spectral control generally applied in the study of zeolites was used for characterization of the nature, strength and total (in micropores and on mesopore surface) concentration of acid sites [29]. The thin plates of the studied samples (8 – 12  $\text{mg}/\text{cm}^2$ , without binder) were placed in a cuvette with NaCl windows and evacuated ( $P = 1.4$  Pa) at 400 °C for 1 h; pyridine was adsorbed at 150 °C for 15 min, and desorbed at 150 – 400 °C (step 50 °C, holding time 30 min). The concentration of Lewis (L-sites) and Brønsted (B-sites) acid sites was determined from the integral intensity of the absorption bands at 1454  $\text{cm}^{-1}$  and 1545  $\text{cm}^{-1}$  respectively using the integral molar absorption coefficients for these bands:  $\varepsilon(\text{L}) = 2.22$   $\text{cm}/\mu\text{mol}$  and  $\varepsilon(\text{B}) = 1.67$   $\text{cm}/\mu\text{mol}$  [30].

Method of 2,4,6-tri-*tert*-butylpyridine (TTBPy) ad(de)sorption with IR-spectral control [31] was used for study the accessibility of Brønsted acid sites for bulky molecules. The technique of the experiment is similar to the method described above for pyridine ad(de)sorption. 2,4,6-tri-*tert*-butylpyridine was adsorbed at 150 °C (in a cuvette with a sample) for 1 h. The adsorption process last a longer time in comparison with the pyridine adsorption since TTBPy is solid under room temperature.

The acid properties of the samples were also investigated by the standard method of temperature-programmed desorption of ammonia (TPDA) [32]. The sample was activated for 30 min in a flow of helium at 550 °C (heating rate to a given temperature was 15 °C/min), cooled to 100 °C and saturated with ammonia for 20 min; physically bound  $\text{NH}_3$  was desorbed by purging with helium at 100 °C. The residual  $\text{NH}_3$  was desorbed by heating in the temperature range of 100 – 700 °C (15 °C/min) and the positions of the desorption maxima were determined using chromatograph LHM-80 (thermal conductivity detector) and recorded as a TPDA curve. The total amount of desorbed ammonia was determined by titrating with  $1 \cdot 10^{-3}$  M hydrochloric acid solution using automatic titrating burette. The peak positions of thermal desorption of  $\text{NH}_3$  were determined by deconvolution of TPDA curves using the Gaussian-type peak shape.

### 2.3 Catalytic measurements

The tetrahydropyranylation reaction of alcohols (1-hexanol, 1-octadecanol and 1-adamantanemethanol) with 3,4-dihydro-2*H*-pyran (DHP) was performed in the liquid phase at 60 °C or 75 °C under atmospheric pressure in a multi-experiment workstation StarFish (Radleys

Discovery Technologies). Prior to the experiment, the catalyst in H-form (50 mg) was activated at 450 °C for 90 min with a heating rate of 2 °C/min. For the tetrahydropyranylation of 1-hexanol, 10 ml of hexane (solvent, Alfa Aesar, 99 %), 0.4 g of mesitylene (internal standard, Alfa Aesar, 98 %), 1.032 g (10 mmol) of 1-hexanol (Alfa Aesar, 99 %) and the catalyst (50 mg) were placed in a threenecked vessel equipped with a condenser and a thermometer. After the solution reached the reaction temperature (60 °C), the DHP (1.275 g, 15 mmol, Sigma Aldrich, 99 %) was added into the vessel. Samples of the reaction mixture were taken periodically and analyzed using 7890B GC (Agilent) equipped with a non-polar HP-5 column (length 30 m, diameter 0.320 mm, and film thickness 0.25 µm, Agilent) and flame ionization detector. The reaction products were identified by using a Thermo Scientific® ISQ LT – TRACE 1310 GC/MS. In the case of the tetrahydropyranylation of 1-octadecanol, 10 ml of DHP (also as solvent), 0.4 g of mesitylene and the catalyst (50 mg) were placed in a vessel, and after the solution reached the reaction temperature (75 °C), 1-octadecanol (0.541 g, 2 mmol, Sigma Aldrich, 99 %) was added. For the tetrahydropyranylation of 1-adamantanemethanol, 0.5038 g (3 mmol, Acros Organics, 99 %) of this alcohol, 10 ml of DHP and 0.4 g of mesitylene were placed in a vessel, and after the solution reached the reaction temperature (75 °C), catalyst (50 mg) was added.

The conversion of alcohols was calculated based on the amount of converted alcohol reactants using an internal standard. ‘The number of converted reactant alcohol molecules per total acid sites’ per unit time (h) (*i. e.* turnover frequency, ‘TOF’) and ‘total number of reactant molecules converted per acid sites’ during 24 h (*i. e.* turnover number, ‘TON’) based on the total concentration of both Brønsted and Lewis acid sites accessible for pyridine molecules.

### 3. Results and discussion

#### 3.1 Influence of the duration of hydrothermal treatment on the structure and acid properties of hierarchical Beta zeolites

To investigate the influence of the duration of hydrothermal treatment on the textural and acid properties of hierarchical Beta zeolite, the synthesis time was varied (1 – 9 days) at constant H<sub>2</sub>O/Si molar ratio in the gel (2.5) and temperature of the synthesis (140 °C, Table 1). The hydrothermal treatment for 1 day leads to the formation of the low-crystalline sample (MB-1,  $\alpha_{\text{cryst}} = 0.15$ , Figs. 1 and S1). Prolongation of HTT up to 2 days results in the formation of partially crystalline material (sample MB-2), consisting of fused Beta zeolite nanoparticles with a size of 40 – 60 nm (according to TEM and SEM data, Figs. 1b and S2). The further increase in the duration of HTT to 7 days results in an increase in the degree of crystallinity determined by change in the integral intensities of the peaks in the  $2\theta = 20 - 24^\circ$  range in the XRD patterns of the sample (Table S1, MB-4). The electron diffraction (ED) for the sample MB-4 (Fig. 1c, inset) confirms the crystal structure of this sample. Sample MB-4 consists of Beta nanoparticles (30 – 40 nm, Fig. 1) smaller in comparison with the sample MB-2. The size for MB-4 is also significantly lower than that of Beta zeolite (ca. 0.2 µm, Fig. S3) obtained under similar conditions using diluted RM (H<sub>2</sub>O/Si = 20). Relatively small size of the particles obtained in highly concentrated RM can be explained by the formation of large number of zeolite nuclei (during the crystallization step), which can easily agglomerate resulting in the dense packing of the particles preventing their further growth [21,33]. Prolongation of HTT to 9 days leads to the growth of zeolite nanoparticles up to 50 – 70 nm (sample MB-5, Figs. S2 and S4).

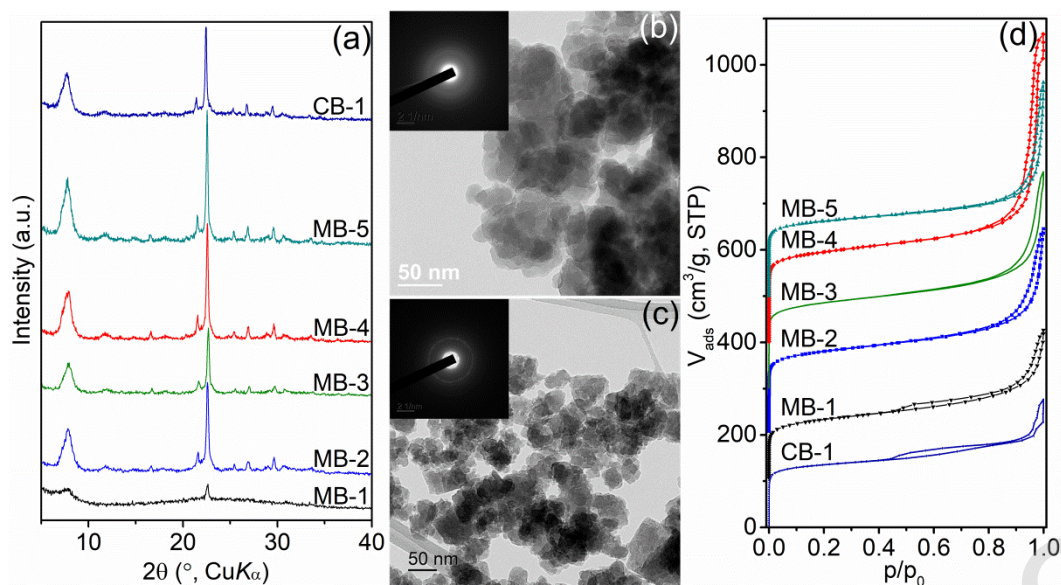


**Fig. 1.** XRD patterns (a) of the as-synthesized samples MB-1 – 5 and CB-1. TEM images of the samples MB-2 (b) and MB-4 (c). *Inset* (b), (c) the ED patterns of the samples MB-2 and MB-4, respectively. Nitrogen ad(de)sorption isotherms (d) at  $-196$  °C for the samples MB-1 – 5 and CB-1. The isotherms of the samples MB-1 – 5 were vertically offset by  $100$  cm<sup>3</sup>/g relative to each other.

Nitrogen ad(de)sorption isotherms ( $-196$  °C) for the samples MB-1 – 5 (Fig. 1) are referred to type IV (according to IUPAC classification). Porous system of these samples includes micropores ( $V_{\text{micro}} = 0.17 - 0.25$  cm<sup>3</sup>/g,  $D_{\text{micro}} = 0.65$  nm, Table 2) similar to Beta zeolite obtained in diluted RM (CB-1). The obtained materials also contain interparticle mesopores ( $V_{\text{meso}} = 0.29 - 0.69$  cm<sup>3</sup>/g,  $S_{\text{meso}} = 85 - 130$  m<sup>2</sup>/g) in contrast to the sample CB-1. Prolongation of HTT from 1 to 7 days is accompanied by an increase in the micropore and mesopore volumes, mesopore surface area and  $S_{\text{BET}}$ . For the sample MB-5 an increase in the nanoparticles size is accompanied by a deteriorating of the textural properties of the sample (Table 2).

The acid properties of partially crystalline materials MB-2, MB-4 and MB-5 (Si/Al ratio of 27 – 31, Table S2) were characterized by the methods of pyridine ad(de)sorption with IR-spectral control and TPDA. According to the data of pyridine ad(de)sorption with IR-spectral control, an increase in the crystallization time to 7 – 9 days leads to an increase in the total concentration of medium and strong Brønsted acid sites (pyridine remains after desorption at  $250$  °C) in the obtained samples ( $72 \rightarrow 88$   $\mu\text{mol/g}$ , Fig. S6; Table S2), as well as the ratio of concentrations of Brønsted and Lewis acid sites ( $1.5 \rightarrow 2.1$ ), that is also due to an increase in the degree of crystallinity of the samples. According to TPDA data (Fig. S7; Table S3) the samples MB-2, MB-4 and MB-5 contain medium and strong acid sites ( $\text{NH}_3$  desorption maximum at  $340 - 370$  °C) similarly to CB-1 (Si/Al = 20). With an increase in the duration of HTT from 2 days (sample MB-2) to 9 days (sample MB-5), the concentration of these acid sites increases ( $133 \rightarrow 240$   $\mu\text{mol/g}$ ), which can be related to the higher degree of crystallinity of the MB-5 sample (Tables S1 and S3).

To estimate the accessibility of Brønsted acid sites for the bulky molecules (larger than the micropore size of Beta zeolite), as well as the strength of the highly-accessible sites, the method of 2,4,6-tri-*tert*-butylpyridine (TTBPy) ad(de)sorption is used. 2,4,6-Tri-*tert*-butylpyridine can interact only with the Brønsted acid sites located on the external or mesopore surface because its molecule

is too large to enter 12-MR pores of Beta. The absorption band at  $3370\text{ cm}^{-1}$  corresponding to the vibrations of  $\equiv\text{N-H}^+$  of protonated TTBPY is present in IR spectra of the samples MB-2, MB-4 and MB-5 (Fig. S8) recorded after TTBPY adsorption at  $150\text{ }^\circ\text{C}$  followed by its desorption at  $150 - 450\text{ }^\circ\text{C}$ . Integral intensity of this band is proportional to the concentration of Brønsted acid sites on the mesopore surface of the samples. Absorption band at  $3610\text{ cm}^{-1}$  corresponds to the stretching vibration of O-H bonds in acid bridging SiOHAl-groups. Its intensity is decreased as a result of TTBPY interaction with the highly-accessible B-sites of the obtained samples (Fig. S8). Integral intensities of the absorption band at  $3370\text{ cm}^{-1}$  for the samples MB-2, MB-4 and MB-5 are 2.1 – 2.7 times higher than those of the sample CB-1 (Table S4) with small external surface area ( $40\text{ m}^2/\text{g}$ ). The samples MB-4 and MB-5 with a degree of crystallinity of 0.75 – 1.0 are characterized by a larger fraction of strong Brønsted acid sites (TTBPY remains after desorption at  $350\text{ }^\circ\text{C}$ ) on the mesopore surface (0.53 – 0.71, Table S5) compared to MB-2 with  $\alpha_{\text{cryst}}$  of 0.6 (0.50).

### 3.2 Influence of the $\text{H}_2\text{O}/\text{Si}$ ratio in the reaction mixture on the structure and acid properties of hierarchical Beta zeolites

To study the influence of water content in the RM on the textural and acid properties of the obtained aluminosilicates, mixtures with the  $\text{H}_2\text{O}/\text{Si}$  ratios of 1 – 14 (Table 1) were subjected to HTT at  $140\text{ }^\circ\text{C}$  for 7 days. The sample MB-6 obtained at the lowest water content ( $\text{H}_2\text{O}/\text{Si} = 1$ ) is X-ray amorphous (Fig. S9). With an increase in the  $\text{H}_2\text{O}/\text{Si}$  ratio in RM from 2.5 to 5.5, the crystallite size of Beta zeolite decreases from 35 to 15 nm (samples MB-4 and MB-8, Figs. 1c and 2a). A further increase in the  $\text{H}_2\text{O}/\text{Si}$  ratio to 14.0 leads to an increase in the zeolite crystallite size from 14 to 22 nm (calculation by the Scherrer's equation) and some decrease (Table S1) in the degree of crystallinity.

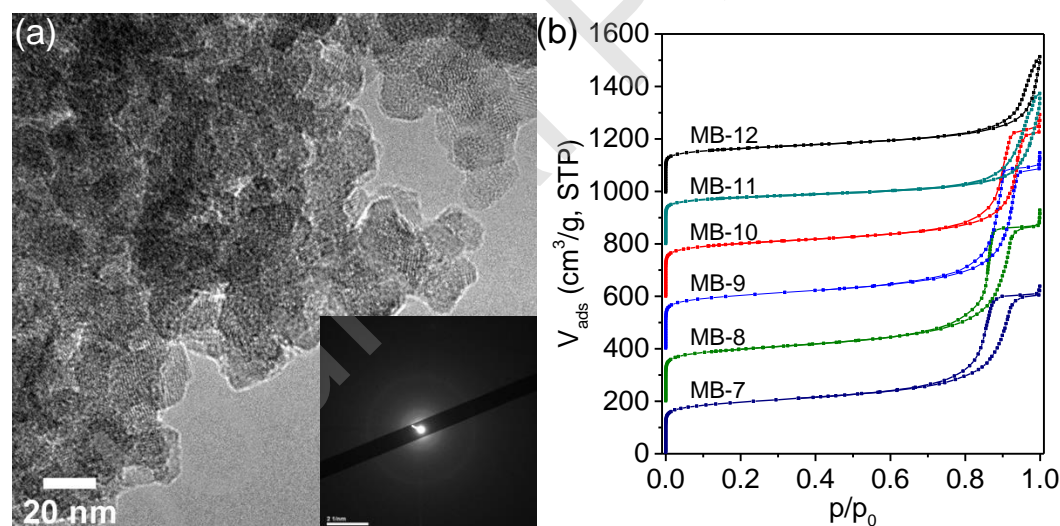


**Fig. 2.** TEM images (a) of the sample MB-8. *Inset* (a) the ED pattern of the sample MB-8. Nitrogen ad(de)sorption isotherms (b) at  $-196\text{ }^\circ\text{C}$  for the samples MB-7 – 12. The isotherms of the samples MB-8 – 12 were vertically offset by  $200\text{ cm}^3/\text{g}$  relative to each other.

According to the data of nitrogen ad(de)sorption at  $-196\text{ }^\circ\text{C}$  (Fig. 2), the sample MB-8 obtained at  $\text{H}_2\text{O}/\text{Si}$  ratio in the gel of 5.5 is characterized by the higher mesopore volume ( $0.81\text{ cm}^3/\text{g}$ ) and surface area ( $230\text{ m}^2/\text{g}$ ), as well as mesopore size uniformity ( $D_{\text{meso}} = 15 \pm 1.0\text{ nm}$ , Fig.

S10), in comparison with the samples obtained at lower or higher H<sub>2</sub>O/Si ratio in the RM (Table 2). It can be assumed, that an optimal ratio is reached between the dissolution and crystallization rates at the H<sub>2</sub>O/Si ratio of 5.5 and the corresponding alkalinity, which promotes the formation of nanoparticles with uniform size and thus a highly porous structure after their assembly [21].

**Table 2**

Characteristics of porous structure (N<sub>2</sub>, -196 °C) of the samples obtained at the different H<sub>2</sub>O/Si ratio in the reaction mixture.

Sample	$V_{\text{micro}}$ (cm <sup>3</sup> /g)	$V_{\text{meso}}$ (cm <sup>3</sup> /g)	$D_{\text{meso}}$ (nm)	$S_{\text{meso}}$ (m <sup>2</sup> /g)	$S_{\text{BET}}$ (m <sup>2</sup> /g)
MB-7	0.21	0.71	14.2	215	730
MB-8	0.21	0.81	15.4	230	765
MB-9	0.23	0.84	19.4	200	780
MB-10	0.25	0.73	21.9	175	780
MB-11	0.24	0.62	25.3	105	690
MB-12	0.22	0.59	42.0	125	650

The optimized samples MB-8 (H<sub>2</sub>O/Si = 5.5) and MB-9 (H<sub>2</sub>O/Si = 7.0) are characterized by the similar concentrations of medium and strong Brønsted acid sites (114 – 138 μmol/g, Py remains after desorption at 250 °C, Table S2). Accessibility of these sites for TTBPY is 3.8 – 4.1 times higher in comparison with the sample CB-1 (Table S4).

### 3.3 Influence of the CTAB/(Si+Al) ratio in the reaction mixture on the structure and acid properties of hierarchical Beta zeolites

To further tune the textural and acid properties of hierarchical zeolites, CTAB was added in the selected RM (up to the CTAB/(Si+Al) ratio of 0.3, samples MB-13 – 22, Figs. S11 and S12). With an increase in CTAB/(Si+Al) ratio in the RM from 0.01 to 0.2, the particle size of zeolite increases from 35 nm to 0.4 μm (Table S1, Fig. S13). It can be assumed, that the presence of positively charged micelles CTAB in RM (at the CTAB/(Si+Al) ratio of 0.01 – 0.2) cause the aggregation of the negatively charged silica particles (flocculation effect), that is also observed in the presence of a cationic polymer [34]. The amorphous fibrous phase appears in the sample MB-20 (Fig. S14) at the CTAB/(Si+Al) ratio in the RM is 0.225. The fraction of this amorphous phase increases with an increase in the concentration of CTAB (samples MB-20 and 21, Fig. S14). After the ratio reaches 0.3 (sample MB-22), the material consists of amorphous particles with size of 5 – 10 nm (Fig. 3). The absorption band at 570 cm<sup>-1</sup> corresponding to the asymmetric stretching vibrations of (alumino)siloxane bonds in five- and six-membered rings of Si(Al)O<sub>4/2</sub> tetrahedra in secondary building units of Beta zeolite [35,36] is present in IR spectrum of the MB-22 sample (Fig. S15). This absorption band does not appear in the spectrum of amorphous AlSi-MCM-41. The micelles of CTAB at the high CTAB/(Si+Al) ratio additionally limit the growth of zeolite nanoparticles during hydrothermal treatment of concentrated reaction mixtures. Thus, sample MB-22 consists of small Beta nanoparticles (less than 10 nm).

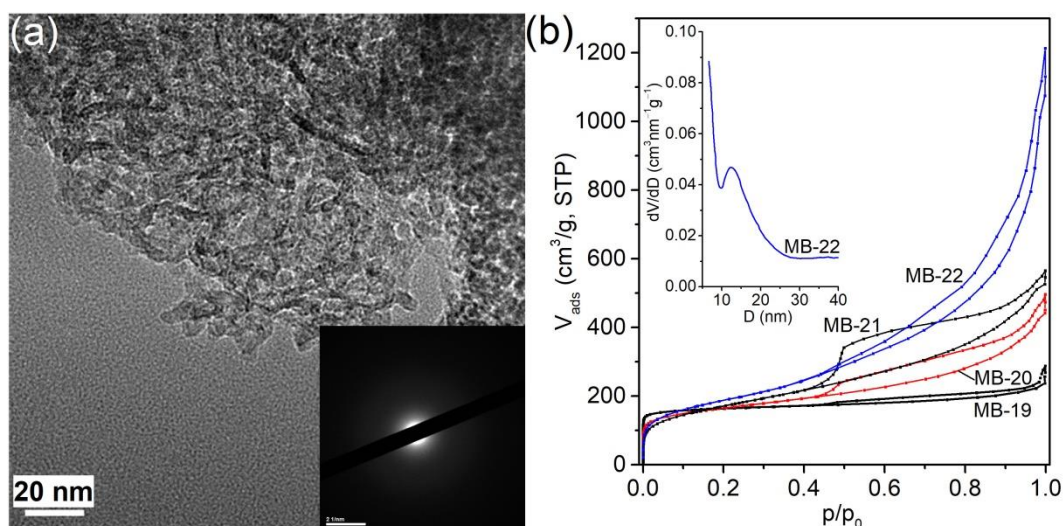


**Fig. 3.** TEM images (a) of the sample MB-22. *Inset* the ED of the samples. Nitrogen ad(de)sorption isotherms (b) at  $-196\text{ }^{\circ}\text{C}$  for the samples MB-19 – 22. *Inset* mesopore size distribution (from the desorption branch) curves for the sample MB-22.

Nitrogen ad(de)sorption isotherms of the samples MB-13 – 22 obtained in the presence of CTAB are given in Figs. 3 and S16. The absence of the steep nitrogen uptake in the mesopore region of isotherms for samples MB-18 – 22 indicates a wider mesopore size distribution of these samples, compared to MB-13 – 17. With an increase in the CTAB/(Si+Al) ratio from 0.05 to 0.2, the mesopore volume and surface area decrease (Table 3), due to an increase in the zeolite particle size. A further increase in CTAB/(Si+Al) from 0.225 to 0.3 promotes an increase in these parameters and a decrease in the micropore volume. The use of concentrated RMs, which additionally contain CTAB (CTAB/(Si+Al) = 0.225 – 0.3) limiting the crystallites growth, contributes to the formation of hierarchical Beta zeolites with a larger mesopore surface area (325 – 585  $\text{m}^2/\text{g}$ ), in comparison with previously obtained materials in concentrated media without adding surfactants (235 – 280  $\text{m}^2/\text{g}$ ) [24,25].

**Table 3**

Characteristics of porous structure ( $\text{N}_2$ ,  $-196\text{ }^{\circ}\text{C}$ ) of the samples obtained at the different CTAB/(Si+Al) ratio in the reaction mixture.

Sample	$V_{\text{micro}}$ ( $\text{cm}^3/\text{g}$ )	$V_{\text{meso}}$ ( $\text{cm}^3/\text{g}$ )	$D_{\text{meso}}$ (nm)	$S_{\text{meso}}$ ( $\text{m}^2/\text{g}$ )	$S_{\text{BET}}$ ( $\text{m}^2/\text{g}$ )
MB-13	0.23	0.85	28.5	155	720
MB-14	0.23	0.82	36.1	130	710
MB-15	0.21	0.83	15.0	205	725
MB-16	0.24	0.55	–	75	660
MB-17	0.23	0.30	–	60	645
MB-18	0.25	0.20	–	50	680
MB-19	0.23	0.14	–	65	640
MB-20	0.11	0.56	–	325	600
MB-21	0.15	0.66	–	375	620
MB-22	0.03	1.66	12.0	585	690

To investigate the state of Al in the samples obtained under optimal conditions (either in the presence or absence of CTAB),  $^{27}\text{Al}$  MAS NMR spectra were collected (Fig. S17). The peaks at 54

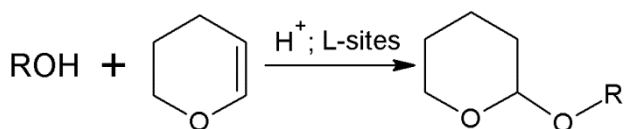
ppm and 0 ppm are associated to aluminum atoms in the tetrahedral (the atoms in zeolite framework) and octahedral (extraframework Al species) coordination environment, respectively [37]. Because of the higher content of amorphous phase, the sample MB-20 obtained in the presence of CTAB is characterized by the higher fraction of Al atoms in octahedral coordination environment compared to MB-8, prepared from CTAB-free mixture.

With an increase in the CTAB/(Si+Al) ratio from 0.05 to 0.2, the concentration of acid sites, as well as the fraction of strong Brønsted acid sites in the samples increase (65 → 481  $\mu\text{mol/g}$  and 0.43 → 0.60, Tables S3 and S2, respectively). A further increase in the CTAB concentration leads to a decrease in the acid sites concentration in the samples (481 → 175  $\mu\text{mol/g}$ ), that can be associated with a decline in the degree of crystallinity of the materials. The appearance of the minimum at 0.2 for the dependence of accessibility of Brønsted acid sites for TTBPY molecules on CTAB/(Si+Al) ratio in the RM (Table S4) is caused by the change in the mesopore surface area of the obtained samples (Table 3).

The use of multi-quaternary ammonium surfactant is a known method for synthesis of hierarchical zeolites, but expensive one. Here we propose a cheaper and simpler method based on the use of concentrated reaction mixtures and CTAB for preparation of similar materials. The reference sample NS-1 obtained in the presence of surfactant  $[\text{C}_{22}\text{-6Npipe-C}_{22}](\text{OH}^-)_6$  consists of Beta nanoparticles with size of ca. 10 – 20 nm (Fig. S18 and S19). The nanoparticles are randomly interconnected forming a nanosponge-like assembly similar to the hierarchical Beta zeolites obtained in concentrated RM (Fig. 2). The porous system of nanosponge Beta zeolite includes micropores (Table S6) and interparticle mesopores with size of 4.5 nm (Fig. S20) formed between agglomerated nanoparticles. Lewis to Brønsted acid sites ratio in the sample HB (Si/Al = 15) is 4 (Table S2), that can be associated with the increased concentration of the defect Lewis sites in the hierarchical Beta nanosponge zeolite [26]. Commercial Beta zeolite (XRD pattern of the sample CB-2 is shown in Fig. S18) contains micropores (Table S6, Fig. S20) and is characterized by significant fraction of Al atoms in octahedral coordination environment (Fig. S17).

### 3.4 Catalytic activity of hierarchical Beta zeolites in tetrahydropyranylation of alcohols

Tetrahydropyranylation of alcohols (Scheme 1) is used to protect hydroxyl group or to obtain respective ethers, important intermediates in organic synthesis [26,38]. Reaction occurs on both Brønsted and Lewis acid sites, while zeolites are widely used as catalysts due to their tunable acidity, high structural stability and easy regeneration [26]. At the same time, the interaction of 3,4-dihydro-2H-pyran (DHP) with bulky alcohols in zeolite micropores is spatially limited and occurs mainly on the mesopore surface of the catalyst particles. Therefore, hierarchical zeolites with a developed mesopore surface are promising catalysts for these reactions [26,39,40]. 1-Hexanol, 1-octadecanol and 1-adamantanemethanol were used as reactants to distinguish the activity and accessibility of acid sites in designed materials. In contrast to 1-hexanol, diffusion of relatively large 1-octadecanol, 1-adamantanemethanol and respective products in micropores of Beta framework is expected to be limited. The selectivity towards tetrahydropyranyl ether in the reactions of DHP with alcohols is ca. 100 % for all catalysts studied (formation of DHP oligomers with no alcohol molecules participating in this side reaction is not taken into account).



**Scheme 1.** Tetrahydropyranylation of alcohols with DHP over acid catalysts.

High conversion of 1-hexanol (almost 100 % after several minutes of the reaction, Figs. 4 and S21) in its reaction with DHP is achieved using MB materials characterized by a significant fraction of highly-accessible acid sites (Table S4). For the samples MB-17, MB-19, CB-1 and CB-2 (with a lowest mesopore volume and surface area) conversion of 1-hexanol reaches 87 – 95% after 1 h. Due to the larger mesopore volume and surface area, facilitating the diffusion of reagents and reaction products, TOF and TON values for all the obtained hierarchical Beta zeolites exceed the corresponding value for the reference sample CB-2 (Fig. 5). The sample MB-20 with the developed mesoporosity (Table 3) and large fraction of medium and strong Brønsted acid sites accessible for bulky molecules (0.87, Table S5) is characterized by the highest TOF and TON values among the obtained materials (Fig. 5).

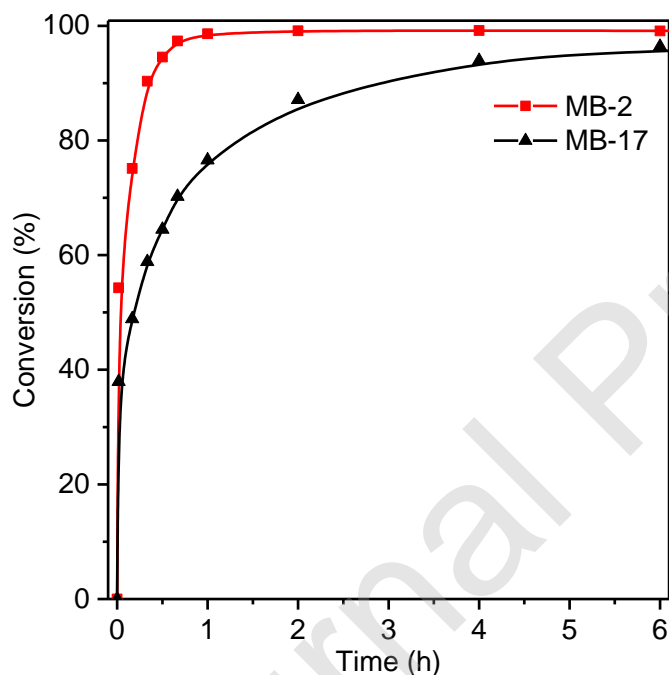


**Fig. 4.** Conversion of 1-hexanol as a function of time in the reaction of 1-hexanol with DHP over the sample MB-2 and MB-17. Reaction conditions: 10 mmol of 1-hexanol, 15 mmol of DHP, 0.4 g of mesitylene (internal standard), 10 ml of hexane (solvent), 50 mg of catalyst, 60 °C.

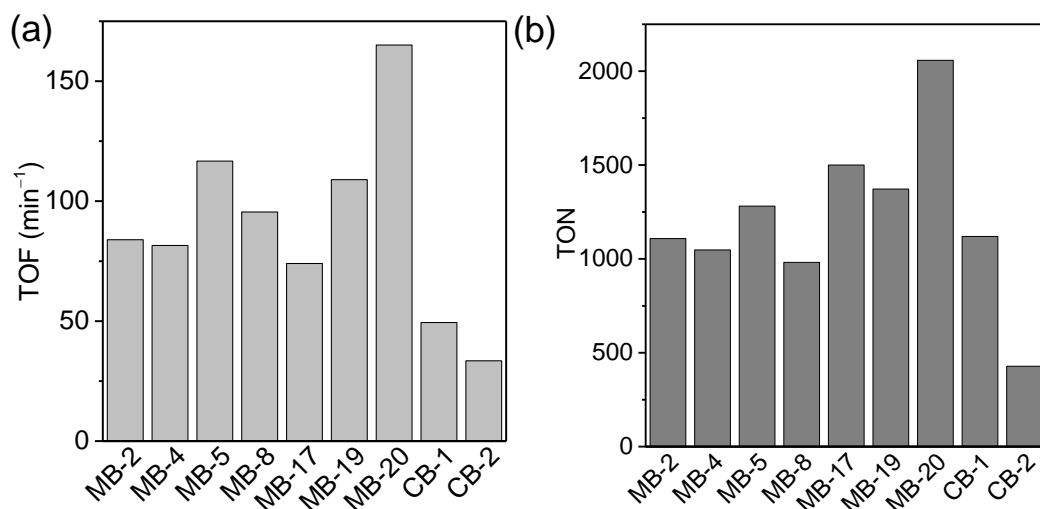


**Fig. 5.** TOF (a) and TON (b) obtained in the reaction of 1-hexanol with DHP over hierarchical Beta zeolites, CB-1 and CB-2. Reaction conditions: 10 mmol of 1-hexanol, 15 mmol of DHP, 0.4 g of mesitylene (internal standard), 10 ml of hexane (solvent), 50 mg of catalyst, 60 °C. Time for TOF calculation is 10 min, TON – 24 h.

With an increase in the carbon chain length in alcohol molecule ( $C_6 \rightarrow C_{18}$ ), the conversion decreases for all the catalysts due to the increased steric hindrance (Fig. 6). The highest value of TOF and TON is achieved using the samples MB-8, 20 – 22 (Fig. 7), because these samples are characterized by the developed mesoporosity (Tables 2 and 3) and the highest accessibility of the acid sites for bulky molecules among the obtained samples (Table S4). The highest conversion of 1-octadecanol (73 % after 24 h) is achieved using the sample MB-8 as a catalyst, characterized by the highest mesopore surface ( $230 \text{ m}^2/\text{g}$ ) and concentration of the acid sites among crystalline samples (Tables 2 and S2). The improved conversion for the samples MB-20 and MB-22 (65 – 67 % for 24 h), compared to MB-21 (43 %), is due to the higher concentration of acid sites in the former materials (Tables S2 and S3). The sample MB-8 consisting of Beta nanoparticles demonstrates higher catalytic activity (in terms of TOF and TON values) compared to the nanosponge Beta zeolite NS-1. This can be associated with the higher fraction of strong Brønsted acid sites in the total acid sites concentration for MB-8 (0.31, for the samples NS-1 is 0.06, Table S2), because these sites are apparently more active in the reaction, than weak and medium Brønsted acid sites and Lewis acid sites.

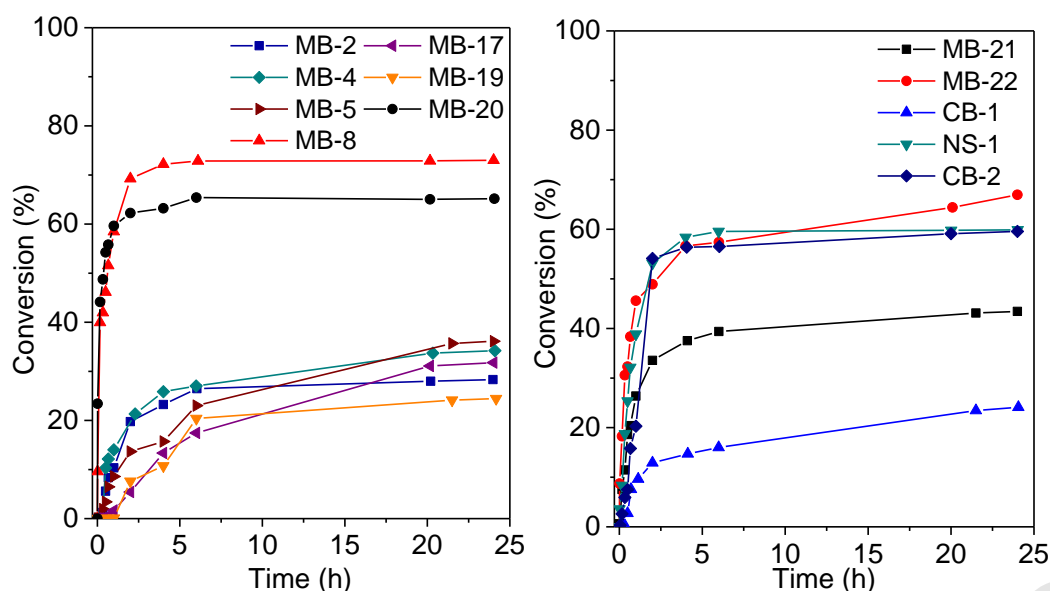


**Fig. 6.** Conversion of 1-octadecanol as a function of reaction time in the reaction of 1-octadecanol with DHP over the obtained and reference samples. Reaction conditions: 2 mmol of 1-octadecanol, 10 ml of DHP, 0.4 g of mesitylene (internal standard), 50 mg of catalyst, 75 °C.

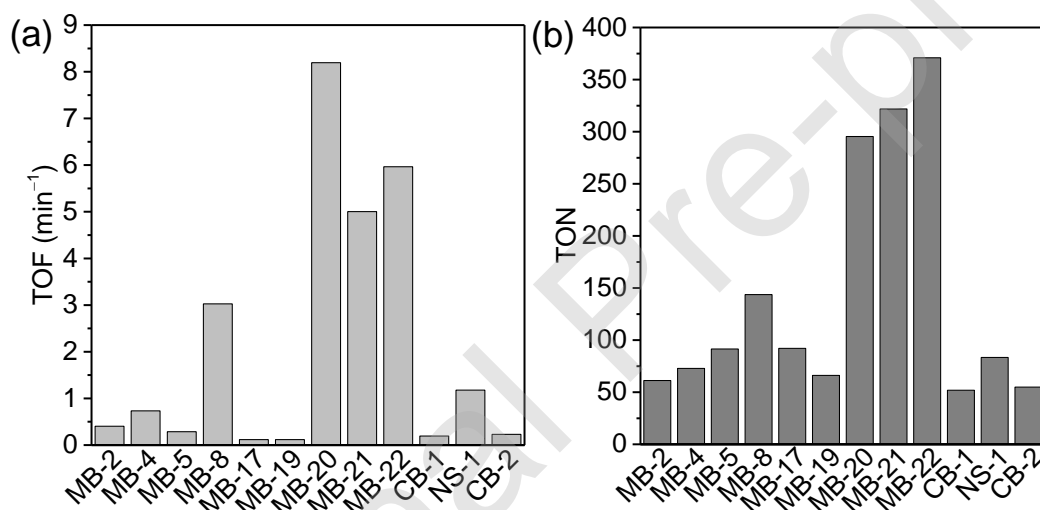


**Fig. 7.** TOF (a) and TON (b) obtained in the reaction of 1-octadecanol with DHP over hierarchical Beta zeolites and reference samples. Reaction conditions: 2 mmol of 1-octadecanol, 10 ml of DHP, 0.4 g of mesitylene (internal standard), 50 mg of catalyst, 75 °C. Time for TOF calculation is 30 min, TON – 24 h.

The highest conversion of bulky 1-adamantanemethanol (83 % after 24 h, Fig. 8) is achieved using X-ray amorphous nanosized MB-22, as well as the samples MB-8, MB-21 and NS-1 (75 – 89 % conversion) because these samples have the largest mesopore surface area (230 – 580 m<sup>2</sup>/g) and high accessibility of the acid sites. As in the case of the reaction DHP with 1-octadecanol, the highest TOF and TON values for the samples MB-21 and MB-22 (Fig. 9) can be associated with the high fraction of the acid sites on the mesopore surface (Table S4).

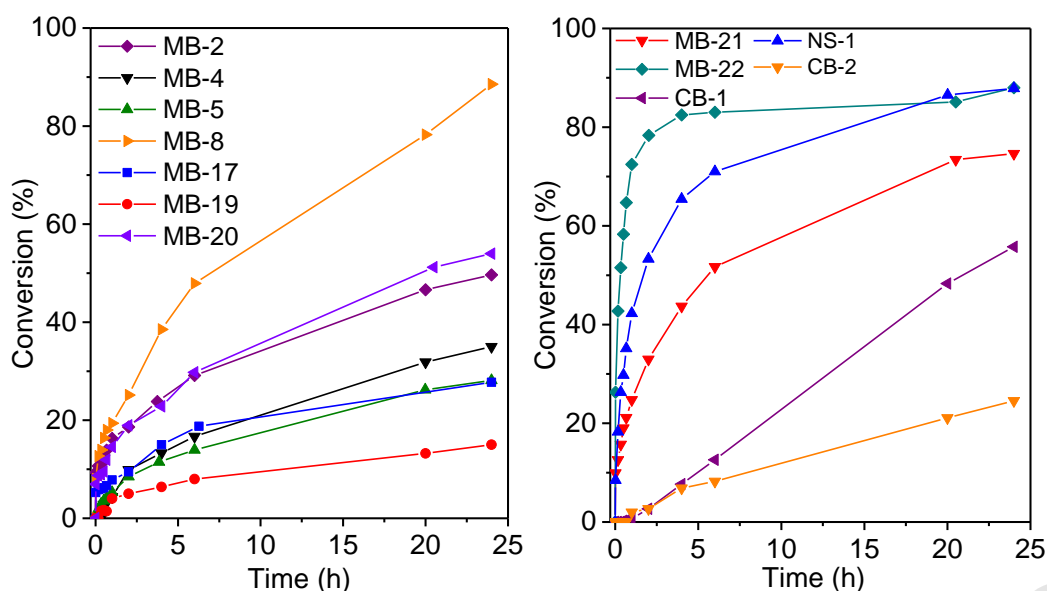


**Fig. 8.** Conversion of 1-adamantanemethanol as a function of time in the reaction of 1-adamantanemethanol with DHP over the obtained and reference samples. Reaction conditions: 3 mmol of 1-adamantanemethanol, 10 ml of DHP, 0.4 g of mesitylene (internal standard), 50 mg of catalyst, 75 °C.

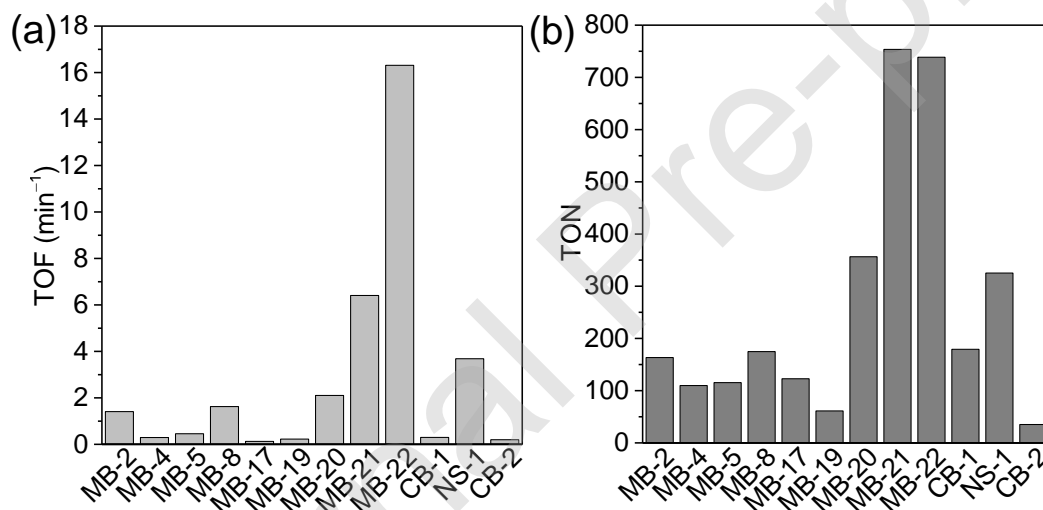


**Fig. 9.** TOF (a) and TON (b) obtained in the reaction of 1-adamantanemethanol with DHP over hierarchical Beta zeolites and reference samples. Reaction conditions: 3 mmol of 1-adamantanemethanol, 10 ml of DHP, 0.4 g of mesitylene (internal standard), 50 mg of catalyst, 75 °C. Time for TOF calculation is 30 min, TON – 24 h.

In order to study structure – activity relationship we have tried to correlate TOF values with particular parameters of acidity and/or accessibility crucial for each reactant type. For elucidating the trends, the samples obtained in the frame of one synthesis set (see section 3.3) were used for comparison. For 1-hexanol, with an increase in the fraction of accessible for pyridine strong Brønsted acid sites in the samples obtained in the presence of CTAB (CTAB/(Si+Al) = 0.05 – 0.225), TOF linearly increases (Fig. 10a). For the reaction of DHP with a larger molecule (1-octadecanol), TOF increases with an increase in the fraction of medium Brønsted acid sites accessible for TTBPpy molecules (Fig. 10b) in the samples obtained at CTAB/(Si+Al) = 0.2 – 0.3 in

the RM. An increase in the fraction of accessible medium Brønsted acid sites with a rise of CTAB/(Si+Al) ratio from 0.2 to 0.3 can be related to a formation of amorphous fibrous phase with a developed mesopore surface and decrease in the degree of crystallinity of the obtained samples. In the case of the most bulky 1-adamantanemethanol, TOF increases with a rise of the fraction of accessible Brønsted acid sites for TTBPY of the samples obtained at CTAB/(Si+Al) = 0.2 – 0.3 (Fig. 10c). This observation can be explained by the fact that the accessibility of acid sites increases with an increase in the concentration of CTAB in the RM, the micelles of which limit the growth of zeolite nanoparticles during hydrothermal synthesis.

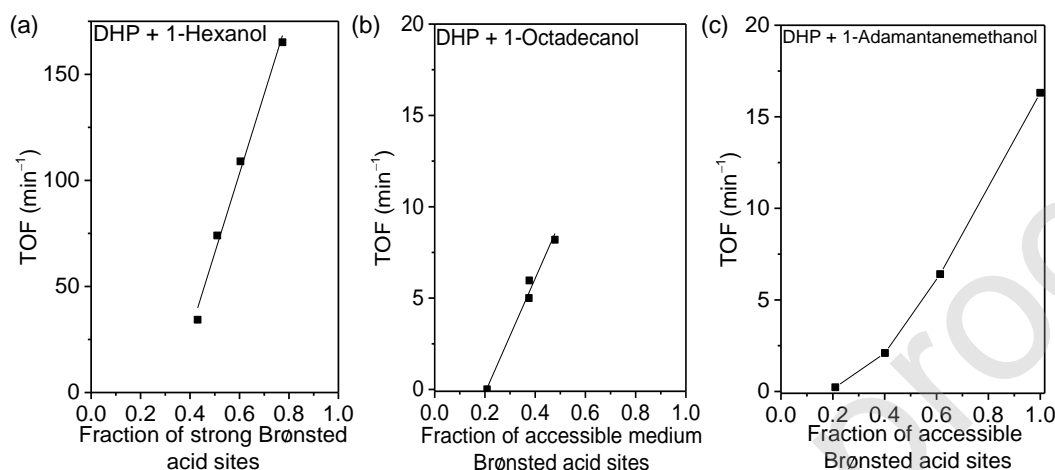


**Fig. 10.** Dependences of TOF on the fraction of strong Brønsted acid sites accessible for pyridine in the catalysts for the reaction of DHP with 1-hexanol (a), fraction of medium Brønsted acid sites accessible for TTBPY in the catalysts for the reaction of DHP with 1-octadecanol (b), fraction of accessible (TTBPY) weak, medium and strong Brønsted acid sites for the reaction of DHP with 1-adamantanemethanol (c). All catalysts were obtained in the presence of CTAB, H<sub>2</sub>O/Si in the RM is 5.5, HTT at 140 °C for 7 days. Reaction conditions are described in the experimental part. Time for TOF calculation is 30 min (for the reaction of DHP with 1-hexanol is 10 min).

## Conclusions

Hierarchical zeolites consisting of Beta nanoparticles (15 – 40 nm in size) were obtained via hydrothermal treatment of a concentrated Beta zeolite gel-precursor (H<sub>2</sub>O/Si = 2.5 – 14). It was found that designed zeolites with increased mesopore volume (up to 0.81 cm<sup>3</sup>/g) and external surface area (up to 230 m<sup>2</sup>/g) can be obtained at the H<sub>2</sub>O/Si ratio in the reaction mixture of 5.5. At this ratio and the corresponding alkalinity, obviously, an optimal balance was reached between the dissolution and crystallization rates, which promoted the formation of small zeolite nanoparticles with uniform size and thus a highly porous structure after their assembly. It was shown that the use of CTAB (with optimum CTAB/(Si+Al) ratio of 0.3) additionally limits the crystallite growth and promotes the formation of X-ray amorphous nanosized aluminosilicate. The obtained materials were characterized by large mesopore volume (up to 1.66 cm<sup>3</sup>/g) and surface area (up to 585 m<sup>2</sup>/g). In the test reactions involving bulky alcohols (1-octadecanol and 1-adamantanemethanol), the highest activity (TOF and TON) was achieved over hierarchical Beta zeolites obtained using high concentration of CTAB in the reaction mixture. The observed increase in catalytic activity of Beta zeolite was related to the improved accessibility of the acid sites for bulky molecules in the designed samples.

### **Author Contributions**

Roman Barakov: synthesis and catalytic testing;

Nataliya Shcherban: synthesis;

Pavel Yaremov: ad/desorption experiments, description of textural properties of designed samples;

Igor Bezverkhyy: advanced characterization of selected samples (TEM, ED);

Valentina Tsyryna: characterization of acidity;

Maksym Opanasenko: catalysis, coordination.

### **Acknowledgement**

RB acknowledges the support of the Czech Science Foundation to the project EXPRO (19-27551X). MO thanks the Primus Research Program of the Charles University (project number PRIMUS/17/SCI/22 “Soluble zeolites”) and OP VVV “Excellent Research Teams” project No.CZ.02.1.01/0.0/0.0/15\_003/0000417– CUCAM.

The authors express their gratitude to Dr. Nikolay Skoryk (“NanoMedTech”, Ukraine), Dr. Sergii Sergiienko (University of Aveiro, Portugal) and Kateryna Filatova (Tomas Bata University in Zlín, Czech Republic) for caring out SEM and some TEM investigations. The authors thank Dr. Zdeněk Tošner (Charles University in Prague) for performing the solid-state MAS NMR studies.

### **Appendix A. Supplementary data**

Supplementary material related to this article can be found at

## References

- [1] E. Koohsaryan, M. Anbia, *Chinese J. Catal.* 37 (2016) 447–467.
- [2] Z. Liu, Y. Hua, J. Wang, X. Dong, Q. Tian, Y. Han, *Mater. Chem. Front.* 1 (2017) 2195–2212.
- [3] A. Feliczak-Guzik, *Microporous Mesoporous Mater.* 259 (2018) 33–45.
- [4] R. Srivastava, *Catal. Today.* 309 (2018) 172–188.
- [5] J. Choi, Z. Wu, A. Yip, W. Khan, X. Jia, *Catalysts* 9 (2019) 127–149.
- [6] T. Pan, Z. Wu, A. Yip, *Catalysts.* 9 (2019) 274–291.
- [7] D. Schneider, D. Mehlhorn, P. Zeigermann, J. Kärger, R. Valiullin, *Chem. Soc. Rev.* 45 (2016) 3439–3467.
- [8] K. Na, G.A. Somorjai, *Catal. Letters.* 145 (2014) 193–213.
- [9] M. Shamzhy, M. Opanasenko, P. Concepción, A. Martínez, *Chem. Soc. Rev.* 48 (2019) 1095–1149.
- [10] D.P. Serrano, J.A. Melero, G. Morales, J. Iglesias, P. Pizarro, *Catal. Rev.* 60 (2018) 1–70.
- [11] W. Schwieger, A.G. Machoke, T. Weissenberger, A. Inayat, T. Selvam, M. Klumpp, A. Inayat, *Chem. Soc. Rev.* 45 (2016) 3353–3376.
- [12] L. Xu, Y. Ma, W. Ding, J. Guan, S. Wu, Q. Kan, *Mater. Res. Bull.* 45 (2010) 1293–1298.
- [13] X. Yin, N. Chu, X. Lu, Z. Li, H. Guo, *Solid State Sci.* 51 (2016) 30–39.
- [14] C. Yin, D. Tian, M. Xu, Y. Wei, X. Bao, Y. Chen, F. Wang, *J. Colloid Interface Sci.* 397 (2013) 108–113.
- [15] T.W. Kim, S.Y. Kim, J.C. Kim, Y. Kim, R. Ryoo, C.U. Kim, *Appl. Catal. B Environ.* 185 (2016) 100–109.
- [16] X. Yan, B. Liu, J. Huang, Y. Wu, H. Chen, H. Xi, *Ind. Eng. Chem. Res.* 58 (2019) 2924–2932.
- [17] Y. Qiu, W. Sun, G. Liu, L. Wang, X. Zhang, *Catal. Letters.* 147 (2017) 1077–1085.
- [18] M.A. Camblor, A. Corma, S. Valencia, *Microporous Mesoporous Mater.* 25 (1998) 59–74.
- [19] A. Petushkov, G. Merilis, S.C. Larsen, *Microporous Mesoporous Mater.* 143 (2011) 97–103.
- [20] G. Majano, S. Mintova, O. Ovsitser, B. Mihailova, T. Bein, *Microporous Mesoporous Mater.* 80 (2005) 227–235.
- [21] K. Möller, B. Yilmaz, R.M. Jacubinas, U. Müller, T. Bein, *J. Am. Chem. Soc.* 133 (2011) 5284–5295.
- [22] J. Zhang, P. Cao, H. Yan, Z. Wu, T. Dou, *Chem. Eng. J.* 291 (2016) 82–93.
- [23] Y. Guo, Z. Zhao, *Chem. Eng. Sci.* 201 (2019) 25–33.
- [24] K. Möller, B. Yilmaz, U. Müller, T. Bein, *Chem. - A Eur. J.* 18 (2012) 7671–7674.
- [25] X. Wang, Y. Li, C. Luo, J. Liu, B. Chen, *RSC Adv.* 3 (2013) 6295–6298.
- [26] H.S. Shin, M. Opanasenko, C.P. Cabello, R. Ryoo, J. Čejka, *Appl. Catal. A Gen.* 537 (2017) 24–32.

- [27] J. Huang, G. Li, S. Wu, H. Wang, L. Xing, K. Song, T. Wu, Q. Kan, *J. Mater. Chem.* 15 (2005) 1055–1060.
- [28] C. Hammond, *The Basics of Crystallography and Diffraction*, third ed., Oxford University Press Inc., New York, 2009.
- [29] K. Kim, R. Ryoo, H.-D. Jang, M. Choi, *J. Catal.* 288 (2012) 115–123.
- [30] C.A. Emeis, *J. Catal.* 141 (1993) 347–354.
- [31] H.K. Heinichen, W.F. Hölderich, *J. Catal.* 185 (1999) 408–414.
- [32] S. Hu, J. Shan, Q. Zhang, Y. Wang, Y. Liu, Y. Gong, Z. Wu, T. Dou, *Appl. Catal. A Gen.* 445–446 (2012) 215–220.
- [33] M.J. Eapen, K.S.N. Reddy, V.P. Shiralkar, *Zeolites*. 14 (1994) 295–302.
- [34] K. Möller, B. Yilmaz, U. Müller, T. Bein, *Chem. Mater.* 23 (2011) 4301–4310.
- [35] E. Masika, R. Mokaya, *Chem. Mater.* 23 (2011) 2491–2498.
- [36] Z. Liu, T. Iida, T. Ikuno, T. Yoshikawa, W. Chaikittisilp, T. Wakihara, T. Okubo, Y. Yanaba, S. Kohara, *J. Am. Chem. Soc.* 137 (2015) 14533–14544.
- [37] A. Petushkov, G. Merilis, S.C. Larsen, *Microporous Mesoporous Mater.* 143 (2011) 97–103.
- [38] T.W. Greene, P.G.M. Wuts, *Protection for the Hydroxyl Group, Including 1,2- and 1,3-Diols, Protective Groups in Organic Synthesis*, John Wiley & Sons, Inc., 2002, pp. 17–245.
- [39] O. Veselý, H. Pang, S.M. Vornholt, M. Mazur, J. Yu, M. Opanasenko, P. Eliášová, *Catal. Today*. 324 (2019) 123–134.
- [40] I. Rodriguez, M.J. Climent, S. Iborra, V. Fornés, A. Corma, *J. Catal.* 192 (2000) 441–447